Coverage Extension of Software Defined Radio Platforms for 3GPP 4G/5G Radio Access Networks

Dereje Mechal Molla
Laboratoire d'informatique Gaspard-Monge
(UMR 8049 LIGM)
ESIEE Paris, Gustave Eiffel University, France
dereje.molla@esiee.fr

Hakim Badis
Laboratoire d'informatique Gaspard-Monge
(UMR 8049 LIGM)
Gustave Eiffel University, France
hakim.badis@univ-eiffel.fr

Laurent George
Laboratoire d'informatique Gaspard-Monge
(UMR 8049 LIGM)
ESIEE Paris, Gustave Eiffel University, France
laurent.george@esiee.fr

Marion Berbineau
COSYS, Gustave Eiffel University
Villeneuve d'Ascq, France
marion.berbineau@univ-eiffel.fr

***Abstract*—The quick development of Software Defined Radio (SDR) platforms has simplified experimenting 3GPP cellular wireless access technologies in software. Thus, many implementations of 3GPP 4G/5G SDR Radio Access Networks (S-RANs) have been developed in the literature. However, most of these S-RANs are tested and evaluated in laboratories within very short-range cells. One of the main reasons for this restricted test environment is the limitation of the output transmit power of SDR devices. The objective of this paper is to show how the cell coverage of 3GPP 4G/5G S-RANs can be extended (numerically and experimentally) to reach a desired cell size such as micro and macro-cells. For this purpose, we first model the communication between user equipment (UE) and eNodeB/gNodeB using an SDR-based radio transceiver in both uplink and downlink directions. Then, we extract the parameters affecting the transmitted and received signal power. After, we numerically analyze the impact of each parameter on the cell coverage. Finally, to validate the numerical analysis, we conduct experiments using a testbed based on an open-source S-RAN implementation to evaluate the transmit power, receive power, Signal-to-Noise Ratio (SNR), and Block Error Rate (BLER). The obtained numerical and experimental results show that different 4G/5G cell sizes can be achieved by using appropriate external equipment including amplifiers, filters, and antennas calibrated according to the employed SDR device specification.**

***Index Terms*—3GPP 4G/5G, cell coverage, Software Defined Radio, S-RAN, transmit power.**

I. Introduction

The 3rd Generation Partnership Project (3GPP) [1] continues to develop technical specifications of cellular mobile communications, and constantly enrich the standards with new features to improve performance and enable new services that are emerging in the market. With the commercial success of the Long Term Evolution (LTE) [2] standard, three classes of use-cases have emerged: enhanced mobile broadband (eMBB), ultra-reliable low-latency communication (URLLC) and massive machine-type communications (mMTC). To support requirements of these use-cases in terms of number of devices, data rates, latency, reliability and energy efficiency, new standards such as LTE-Advanced [3], LTE-Advanced Pro [4] and recently 5G New Radio (NR) [5] are developed. The performance of these solutions, before commercial deployment, have been evaluated by researchers, vendors and operators in laboratories and small-scale real world training environment using open-source or proprietary prototyping platforms.

Several open-source and proprietary implementations of LTE/LTE-A/LTE-A Pro (4G) and 5G NR Radio Access Networks (RANs) based on Software Defined Radio (SDR) platforms have been developed. Examples of such implementations are Software Radio Systems LTE (srsLTE) [6], OpenAirInterface (OAI-RAN) [7], OpenLTE [8], and Amarisoft [9]. The SDR platforms that use these implementations can be named 3GPP 4G/5G SDR-RANs (S-RANs), and can build all the RAN components including eNodeBs/gNodeBs (eNBs/gNBs) and User Equipment (UE). Consequently, the S-RAN cell size provided by eNBs/gNBs is deeply related to the capability of employed SDR devices.

However, most SDR devices recommended by the S-RAN platforms suffer from limited transmit power allowing only short-range wireless communications [10], [11]. This limitation is mainly due to the internal amplifiers and filters of SDR devices. As a result, the performance evaluations of S-RANs reported in many research papers [12]–[14] are generally restricted to short range communications such as in laboratory or in office. To deal with 4G/5G S-RAN cell sizes, our work conducts numerical and experimental analysis going from small-cell (femto, pico, micro) to macro-cell considering different radio propagation models. More specifically, we first model the S-RAN in uplink and downlink communications and perform a numerical analysis to establish an expression for the receive power for each propagation model taking all the parameters affecting the transmit and receive signal power into account. Then, we form a couple of testbeds using an open-source S-RAN implementation to conduct experiments, and measure the performance of our model in terms of the

ISBN 978-3-903176-42-3

transmit power, receive power, Signal-to-Noise Ratio (SNR), and Block Error Rate (BLER), for several test cases varying parameters that impact the cell coverage. Finally, based on the used SDR device capability, we provide optimal specification of additional external equipment such as external amplifiers, filters and low noise amplifiers (LNA) to get the desired indoor/outdoor cell size.

The rest of the paper is organized as follows: section II gives background about 4G/5G RAN coverage requirements, propagation models and S-RAN platforms. Section III discusses the S-RAN model and numerical analysis. Section IV presents experimental testbed, results and performance analysis. Finally, section V concludes the paper and outlines future work.

II. Background Overview

In this section, we provide a brief overview of 3GPP 4G/5G RAN coverage requirements, S-RAN platforms and propagation models.

A. 3GPP 4G/5G RAN coverage requirements

The architecture of 4G/5G cellular network is made up of RAN and core network. The core network is known as Evolved Packet Core (EPC) for 4G and 5G-Core (5GC) for 5G. The RAN is composed of a network of eNBs/gNBs providing coverage to UEs and connectivity to external networks. Each eNB/gNB can cover small-cell or macro-cell area to provide connectivity to UEs in indoor/outdoor urban, suburban or rural areas. The eNBs/gNBs operate in both Frequency Division Duplex (FDD) and Time Division Duplex (TDD) frequency bands, within sub-6GHz licensed spectrum bands and in some portion of the millimeter wave (mmWave) radio spectrum between 24.25 to 52.6GHz for 5G RANs. More detail requirements of each cell type is given in Table I.

TABLE I: RAN coverage requirement.

Parameter	Femto [15]	Pico [16]	Micro [17]	Macro [17]
Frequency	LTE bands; 5G: (3 – 12, 24 – 30, or > 30) GHz			
Bandwidth	LTE: upto 20MHz (CA: 100MHz), 5G: upto 100/400MHz (CA: 800MHz)			
Coverage	<20m	<100m	<1000m	few kms
eNB/gNB TX power	<20dBm	<24dBm	33dBm	46dBm
Ant. gain	0dBi	2dBi	5dBi	15dBi
Modulation	QPSK, 16QAM, 64QAM and 256QAM			
Application	Indoor	(In/Out)door	(In/Out)door	Outdoor

B. Propagation models

Several propagation models related to 4G/5G networks have been developed in literature [16], [18]–[20]. These models consider different parameters such as the desired coverage area cells, deployment area type (urban, rural, indoor/outdoor, *etc.*), operating frequency, *etc*. Table II illustrates the path loss models considered for the four cell types (femto, pico, micro and macro) in 4G/5G under urban, indoor/outdoor and line of sight (LOS) conditions.

The parameters used in Table II are: d is the distance (in meters) between UE and eNB/gNB; f is the carrier frequency in MHz; N is distance power loss coefficient; $P_{\mathrm{f}}(n)$ floor penetration loss factor (dB); n is number of floors between UE and eNB/gNB; P_{i} loss of wall number i; w number of penetrated walls; f_{G} carrier frequency in GHz $(0.5 < f_{\mathrm{G}} < 100GHz)$; d_{BP} is break point distance given by $[4h_{\mathrm{BS}} * h_{\mathrm{UT}} * f/c]$ where $c = 3 \times 10^8 m/s$ is propagation velocity in free space, and h_{BS} and h_{UT} are the effective antenna heights at the eNB/gNB and UE, respectively, where $h_{\mathrm{BS}} \leq 10$m for micro and 25m for macro cell, and h_{UT} is between 1.5m and 22.5m.

TABLE II: Propagation model.

Cell	Path loss [dB] model equations	Deployment	Reference
Femto	$N * \log_{10}(d) + 20\log_{10}(f) + P_{\mathrm{f}}(n) - 28$	Indoor	[18]
Pico	$20\log_{10}(f) + 20\log_{10}(d) - 28 + \sum_{i=0}^{w} P_{\mathrm{i}}$	Indoor	[16]
Micro ($10m \leq d \leq d_{\mathrm{BP}}$)	$22\log_{10}(d) + 28.0 + 20\log_{10}(f_{\mathrm{G}})$	Outdoor; LOS	[19]
Micro ($d_{\mathrm{BP}} \leq d \leq 5km$)	$40\log_{10}(d) + 28.0 + 20\log_{10}(f_{\mathrm{G}}) - 9\log_{10}((d_{\mathrm{BP}})^2 + (h_{\mathrm{BS}} - h_{\mathrm{UT}})^2)$	Outdoor; LOS	[19]
Micro 5G ($10m \leq d \leq d_{\mathrm{BP}}$)	$21\log_{10}(d) + 32.4 + 20\log_{10}(f_{\mathrm{G}})$	Outdoor; LOS	[20]
Micro 5G ($d_{\mathrm{BP}} \leq d \leq 5km$)	$40\log_{10}(d) + 32.4 + 20\log_{10}(f_{\mathrm{G}}) - 9.5\log_{10}((d_{\mathrm{BP}})^2 + (h_{\mathrm{BS}} - h_{\mathrm{UT}})^2)$	Outdoor; LOS	[20]
Macro ($10m \leq d \leq d_{\mathrm{BP}}$)	$22\log_{10}(d) + 28.0 + 20\log_{10}(f_{\mathrm{G}})$	Outdoor; LOS	[19]
Macro ($d_{\mathrm{BP}} \leq d \leq 5km$)	$40\log_{10}(d) + 28.0 + 20\log_{10}(f_{\mathrm{G}}) - 9\log_{10}((d_{\mathrm{BP}})^2 + (h_{\mathrm{BS}} - h_{\mathrm{UT}})^2)$	Outdoor; LOS	[19]

C. S-RAN platforms

The S-RAN platforms have been fully developed as open-source hardware with open-source/proprietary software to perform the whole 4G/5G protocol stack. Among the open-source softwares, the most popular and stable ones providing software implementation of UE, eNB/gNB and EPC are srsLTE [6] and OAI [7]. We use srsLTE in our testbed due to its high modularity, easy customization and supporting complete implementation of UE as a software radio. We also plan to use OAI in future work.

The UE and eNB/gNB in S-RAN are implemented based on SDR platform, where the signal processing functions of lower layers are implemented by software instead of hardware. An SDR platform consists of SDR device, host processor and communication interface. The SDR device incorporates a daughterboard and motherboard to perform analog and digital signal processing functions. In our work we use Universal Software Radio Peripheral (USRP) device from Ettus Research [10] as it is supported by many S-RANs. Most of the USRP devices use AD9361/AD9364 radio frequency integrated circuits (RFICs) covering frequencies upto 6GHz and more than 56MHz bandwidth allowing to support all 4G bands and sub-6GHz 5G bands. They support high speed communication interfaces such as USB, Ethernet and PCIe to allow exchanging data with host processors at high throughput.

III. Numerical coverage analysis of S-RAN

The maximum area covered by UE and eNB/gNB nodes in S-RAN is mostly limited by the transmit power of the used SDR device. In order to extend this coverage, we conduct numerical analysis of S-RAN with different propagation models.

A. S-RAN model and components

Let us consider an S-RAN having one eNB/gNB serving a UE located at a distance R as shown in Fig. 1 both using SDR device. At the transmitter (TX) side (eNB/gNB in downlink [DL] or UE in uplink [UL]), the output signal power is strongly related to SDR device internal amplifier (iAmp), cables and connectors, possible external amplifier (eAmp) and TX antennas. At the receiver (RX) side (UE in DL or eNB/gNB in UL) the received signal power, already

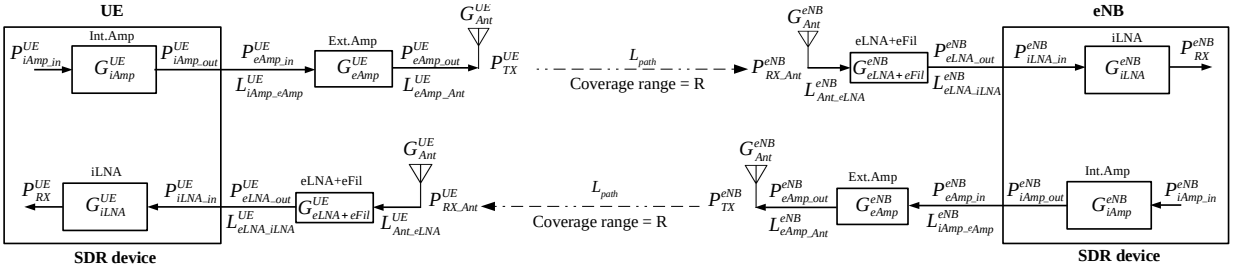

Fig. 1: Uplink and downlink communication in S-RAN.

affected due to the propagation (see Table II), can also be impacted by the RX antenna, possible external LNA with filter (eLNA+eFil), cables, connectors and internal LNA (iLNA).

B. S-RAN coverage analysis

Our objective is to compute the required output TX power for both UL and DL directions ($P_{\mathrm{TX}}^{\mathrm{UE}}$ for UL and $P_{\mathrm{TX}}^{\mathrm{eNB}}$ for DL), and the RX power ($P_{\mathrm{RX}}^{\mathrm{UE}}$ for DL and $P_{\mathrm{RX}}^{\mathrm{eNB}}$ for UL) to get the desired cell size. The expressions for TX and RX powers are given by equations in Table III using the well known link budget analysis with parameters illustrated in Fig. 1 including the path loss ($L_{\mathtt{path}}$). The superscripts $\langle \mathtt{X}, \mathtt{Y} \rangle$ refers $\langle \mathtt{UE}, \mathtt{eNB} \rangle$ in UL and $\langle \mathtt{eNB}, \mathtt{UE} \rangle$ in DL; and PAPR is the Peak to Average Power Ratio. The path loss, $L_{\mathtt{path}}$, varies with the cell type and deployment area and is given by equations in Table II.

TABLE III: Transmit and received power.

Power	Expression
$P^{\mathrm{X}}_{\mathtt{eAmp\_out}}$	$P^{\mathrm{X}}_{\mathtt{iAmp\_in}} + G^{\mathrm{X}}_{\mathtt{iAmp}} - PAPR - L^{\mathrm{X}}_{\mathtt{iAmp\_eAmp}} + G^{\mathrm{X}}_{\mathtt{eAmp}}$
$P^{\mathrm{X}}_{\mathtt{TX}}$	$P^{\mathrm{X}}_{\mathtt{eAmp\_out}} - L^{\mathrm{X}}_{\mathtt{eAmp\_Ant}} + G^{\mathrm{X}}_{\mathtt{Ant}}$
$P^{\mathrm{Y}}_{\mathtt{RX}}$	$P^{\mathrm{X}}_{\mathtt{TX}} - L_{\mathtt{path}} + G^{\mathrm{Y}}_{\mathtt{Ant}} - L^{\mathrm{Y}}_{\mathtt{Ant\_eLNA}} + G^{\mathrm{Y}}_{\mathtt{eLNA+eFil}} - L^{\mathrm{Y}}_{\mathtt{eLNA\_iLNA}} + G^{\mathrm{Y}}_{\mathtt{iLNA}}$
Receiver sensitivity	$\mathtt{thermal\ noise} + \mathtt{noise\ figure} + 10\log_{10}(\mathtt{bandwidth}) + \mathtt{SNR}$

We conduct the numerical analysis using: USRP B210 SDR device with output power @1dB compression [P1dB] = 17.5dBm at 2GHz [10], frequency band 25, PAPR equal to 10dB for UE and 12dB for eNB/gNB [21], and 3dBi antenna gain. The distance, R, between UE and eNB/gNB varies with cell type (see Table I), and for the outdoor scenario UE is assumed to be placed at a height of 1.5m and eNB/gNB at 14m above ground. The RX power in both UL and DL are analyzed for the following four cases: 1) with *no external component* added to B210; 2) *eAmp* added to the TX end; 3) *eLNA+eFil* added to the RX end; and 4) both *eAmp* and *(eLNA+eFil)* added to the TX and RX ends, respectively.

1) Transmit and receive power: The UL and DL TX and RX powers including gains and losses are presented in Table IV and Table V for selected propagation models discussed in section II-B, namely femto and pico cells in indoor, and micro and macro cells in outdoor for case ($d_{\mathrm{BP}} \leq d \leq 5km$).

Table IV and V illustrates that the RX power is very high for all propagation models compared to LTE reference sensitivity level mentioned in the 3GPP technical specification [22]. In particular, the receivers' sensitivity of our model in Fig.1 can also be computed using the expression in Table III. As such, using USRP B210 as the SDR device (with a noise figure of 2.4dB at 2GHz [10]), SNR of (4.6dB for QPSK, 11.3dB for 16QAM and 15.3dB for 64QAM) as stated in LTE standard [22], and a 10MHz LTE signal, the receivers' sensitivity results: -97.3dB for QPSK, -90.3dB for 16QAM and -86.3dB for 64QAM. Thus, the S-RAN model depicted in Fig. 1 can be realized without adding external components to the SDR device, under the selected propagation models stated above, upto one kilometer. However, for larger coverage range, either a high gain antenna or external components are required. In outdoor (micro and macro cells), the final RX power can be improved by using high gain antenna (see Table I). While the effect due to changing the antenna gain is very small in micro cell, for the macro cell using high gain antenna will increase the coverage range upto 3km. Moreover, to use higher bandwidths and modulation techniques in addition to increasing the coverage range, external components need to be employed. This requires to find the appropriate TX power (Z or W) for `eAmp` and gain (G) for `eLNA+eFil` as shown in Table IV and V.

IV. Experimental coverage analysis of S-RAN

To verify the numerical analysis, we conduct experiments using testbeds configured based on the S-RAN model described in section III.

A. Testbed and experiment setup

Two testbeds were setup as shown in Fig. 2. The first testbed corresponds to case 1 of the numerical analysis, *i.e., with no external component*, (see section III-B). The testbed consists of one USRP B210 connected to Miriac LS1046 (ARM Cortex A72 64-bit core processor) from MicroSys at UE and a second USRP B210 device connected to an 8 core Intel x86_64 Core i7 microprocessor (Laptop) at eNB/gNB. Both processors run Linux operating systems (Ubuntu 18.04.2 LTS on the Laptop and a Yocto distribution developed under Yocto project on the Miriac) and srsLTE release_19_06. The B210 devices are connected to the Miriac and Laptop through UHD driver (UHD version UHD_3.14.0.0) via USB 3.0 interface. For both ends, a pair of 3dBi gain vertical omni-directional antennas from Ettus (VERT900 or VERT2450) are connected for full duplex transmission.

The second testbed corresponds to case 2 of the numerical analysis, *i.e., eAmp added to the TX end*, (see section III-B).

TABLE IV: Numerical analysis for UL.

Components	UE (TX)		eNB/gNB (RX)		Path loss (dB)	Final RX power(dBm)
	B210	eAmp	B210	eLNA + eFil		
No external component	$P^{UE}_{iAmp\_out} = 17.5dBm$ $L^{UE}_{iAmp\_Ant} = 0.5dB$ $G^{UE}_{Ant} = 3dBi$ $PAPR = 10dB$	–	$G^{eNB}_{Ant} = 3dBi$ $L^{eNB}_{Ant\_iLNA} = 0.5dB$ $G^{eNB}_{iLNA} = 17dB$	–	76.60(femto) 77.57(pico) 104.50(micro) 116.54(macro)	-47.09 -48.07 -75.00 -87.04
eAmp	$P^{UE}_{iAmp\_out} = 17.5dBm$ $L^{UE}_{iAmp\_eAmp} = 0.5dB$ $G^{UE}_{Ant} = 3dBi$ $PAPR = 10dB$	$\text{Max}P^{UE}_{eAmp\_out} = xdBm$ $\text{EVM}P^{UE}_{eAmp\_out} = ydBm$ $P^{UE}_{eAmp\_out} = \text{Min}\{x - 10dBm, ydBm\} = ZdBm$ $L^{UE}_{eAmp\_Ant} = 0.5dB$	$G^{eNB}_{Ant} = 3dBi$ $L^{eNB}_{Ant\_iLNA} = 0.5dB$ $G^{eNB}_{iLNA} = 17dB$	–	76.60(femto) 77.57(pico) 104.50(micro) 116.54(macro)	$Z - 47.59$ $Z - 48.57$ $Z - 75.50$ $Z - 87.54$
eLNA+eFil	$P^{UE}_{iAmp\_out} = 17.5dBm$ $L^{UE}_{iAmp\_Ant} = 0.5dB$ $G^{UE}_{Ant} = 3dBi$ $PAPR = 10dB$	–	$G^{eNB}_{Ant} = 3dBi$ $L^{eNB}_{Ant\_eLNA} = 0.5dB$ $L^{eNB}_{eLNA\_iLNA} = 0.5dB$ $G^{eNB}_{iLNA} = 17dB$	$G^{eNB}_{eLNA} = G$	76.60(femto) 77.57(pico) 104.50(micro) 116.54(macro)	$G - 47.59$ $G - 48.57$ $G - 75.50$ $G - 87.54$
eAmp and eLNA+eFil	$P^{UE}_{iAmp\_out} = 17.5dBm$ $L^{UE}_{iAmp\_eAmp} = 0.5dB$ $G^{UE}_{Ant} = 3dBi$ $PAPR = 10dB$	$\text{Max}P^{UE}_{eAmp\_out} = xdBm$ $\text{EVM}P^{UE}_{eAmp\_out} = ydBm$ $P^{UE}_{eAmp\_out} = \text{Min}\{x - 10dBm, ydBm\} = WdBm$ $L^{UE}_{eAmp\_Ant} = 0.5dB$	$G^{eNB}_{Ant} = 3dBi$ $L^{eNB}_{Ant\_eLNA} = 0.5dB$ $L^{eNB}_{eLNA\_iLNA} = 0.5dB$ $G^{eNB}_{iLNA} = 17dB$	$G^{eNB}_{eLNA} = G$	76.60(femto) 77.57(pico) 104.50(micro) 116.54(macro)	$W + G - 48.09$ $W + G - 49.07$ $W + G - 76.00$ $W + G - 88.04$

TABLE V: Numerical analysis for DL.

Components	eNB/gNB (TX)		UE (RX)		Path loss (dB)	Final RX power(dBm)
	B210	eAmp	B210	eLNA + eFil		
No external component	$P^{eNB}_{iAmp\_out} = 17.5dBm$ $L^{eNB}_{iAmp\_Ant} = 0.5dB$ $G^{eNB}_{Ant} = 3dBi$ $PAPR = 12dB$	–	$G^{UE}_{Ant} = 3dBi$ $L^{UE}_{Ant\_iLNA} = 0.5dB$ $G^{UE}_{iLNA} = 17dB$	–	76.83(femto) 77.80(pico) 104.73(micro) 116.77(macro)	-49.33 -50.30 -77.23 -89.26
eAmp	$P^{eNB}_{iAmp\_out} = 17.5dBm$ $L^{eNB}_{iAmp\_eAmp} = 0.5dB$ $G^{eNB}_{Ant} = 3dBi$ $PAPR = 12dB$	$\text{Max}P^{eNB}_{eAmp\_out} = xdBm$ $\text{EVM}P^{eNB}_{eAmp\_out} = ydBm$ $P^{eNB}_{eAmp\_out} = \text{Min}\{x - 12dBm, ydBm\} = ZdBm$ $L^{eNB}_{eAmp\_Ant} = 0.5dB$	$G^{UE}_{Ant} = 3dBi$ $L^{UE}_{Ant\_iLNA} = 0.5dB$ $G^{UE}_{iLNA} = 17dB$	–	76.83(femto) 77.80(pico) 104.73(micro) 116.77(macro)	$Z - 49.83$ $Z - 50.80$ $Z - 77.73$ $Z - 89.76$
eLNA+eFil	$P^{eNB}_{iAmp\_out} = 17.5dBm$ $L^{eNB}_{iAmp\_Ant} = 0.5dB$ $G^{eNB}_{Ant} = 3dBi$ $PAPR = 12dB$	–	$G^{UE}_{Ant} = 3dBi$ $L^{UE}_{Ant\_eLNA} = 0.5dB$ $L^{UE}_{eLNA\_iLNA} = 0.5dB$ $G^{UE}_{iLNA} = 17dB$	$G^{UE}_{eLNA} = G$	76.83(femto) 77.80(pico) 104.73(micro) 116.77(macro)	$G - 49.83$ $G - 50.80$ $G - 77.73$ $G - 89.76$
eAmp and eLNA+eFil	$P^{eNB}_{iAmp\_out} = 17.5dBm$ $L^{eNB}_{iAmp\_eAmp} = 0.5dB$ $G^{eNB}_{Ant} = 3dBi$ $PAPR = 12dB$	$\text{Max}P^{eNB}_{eAmp\_out} = xdBm$ $\text{EVM}P^{eNB}_{eAmp\_out} = ydBm$ $P^{eNB}_{eAmp\_out} = \text{Min}\{x - 12dBm, ydBm\} = WdBm$ $L^{eNB}_{eAmp\_Ant} = 0.5dB$	$G^{UE}_{Ant} = 3dBi$ $L^{UE}_{Ant\_eLNA} = 0.5dB$ $L^{UE}_{eLNA\_iLNA} = 0.5dB$ $G^{UE}_{iLNA} = 17dB$	$G^{UE}_{eLNA} = G$	76.83(femto) 77.80(pico) 104.73(micro) 116.77(macro)	$W + G - 50.33$ $W + G - 51.30$ $W + G - 78.23$ $W + G - 90.26$

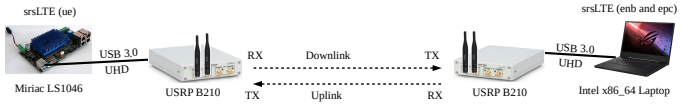

(a) Without external components.

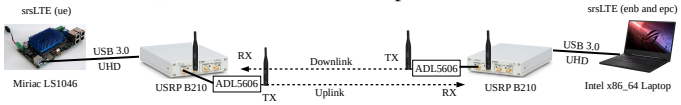

(b) eAmp added to UE and eNB/gNB.

Fig. 2: Experiment testbeds.

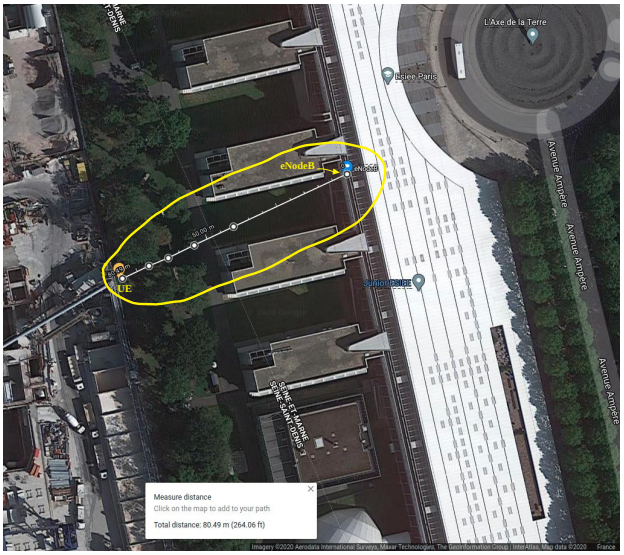

Fig. 3: Outdoor experiment area.

Thus, the testbed is prepared by adding eAmp at the TX end of both UE and eNB/gNB as shown in Fig. 2b. The eAmp used is EVAL-CN0417-EBZ board from Analog Devices [23], which is a USB powered RF power amplifier that uses ADL5606 RF driver amplifier. It operates at 2400MHz frequency band and has 20dB gain and maximum TX power (P1dB) around 29dBm at 2400MHz.

Experiment setup. Our interest is to measure the maximal TX and RX power, SNR and BLER in indoor and outdoor environment. The indoor tests were conducted inside ESIEE Paris building for a distance of upto 12m. Whereas the outdoor tests were conducted outside ESIEE Paris building for a distance of upto 81m placing the UE on a 0.8m height desk and eNB/gNB 14m above ground as shown in Fig. 3. Both indoor and outdoor tests performed in LOS communication. Settings of the parameter used for all measurements include frequency bands: 1800, 1900 and 2450 MHz; bandwidth: 1.4, 3, 5, 10, 15 and 20MHz; UHD gain: 70, 80, and 90dB for TX; and 40 and 76dB for RX. Furthermore, since the eAmp chosen works only at 2400MHz, we performed measurements

of the second testbed based on bandwidth, UHD gain and distance. All TX and RX power measurements are performed using R&S®FSL3 Spectrum Analyzer and SNR is measured from srsLTE trace output.

B. Results and Performance Evaluation

This subsection describes measurement results of TX power, RX power, SNR and BLER.

1) Uplink TX and RX power: The TX power of UE (`srsue`) measured with/without eAmp is illustrated in Table VI. Also shown is the performance of B210 as provided by its vendor [24].

TABLE VI: Transmit power.

UHD Gain (dB)	Frequency (GHz)	TX power (dBm)						
		Measured (dBm)			with eAmp (dBm)			Ettus [24]
		10MHz	15MHz	20MHz	10MHz	15MHz	20MHz	
70	1.8	-24.4	-23.6	-32.5	–	–	–	-3.5
	1.9	-26.9	-23.8	-28.3	–	–	–	-4.0
	2.4	-35.1	-34.4	-34.3	-16.4	-8.2	-16.6	-6.0
80	1.8	-14.6	-14.3	-23.5	–	–	–	5.9
	1.9	-22.8	-14.9	-16.4	–	–	–	5.5
	2.4	-18.9	-24.8	-25.3	-6.7	-1.7	-4.0	4.0
90	1.8	-4.9	-4.0	-6.2	–	–	–	14.5
	1.9	-13.7	-3.0	-6.8	–	–	–	14.0
	2.4	-10.2	-19.2	-14.7	2.1	10.0	8.7	12.0

Without eAmp, the UE's maximum TX power settles below 0dBm at all frequency bands and UHD gains. The maximum is around -3.0dBm much lower than 14dBm as reported by Ettus. This performance difference, in one part is due to the hardware factors as discussed in [25]. On the other hand, it's contributed while executing the full protocol stack of LTE, and PAPR of SC-FDMA used. This is unlike the measurements conducted by Ettus and other researchers [25], [26] where they use single test signals. It's also clearly shown in Table VI that with eAmp the overall TX power has increased to 10dBm, which will help to extend the coverage range.

The RX power at eNB/gNB (`srsenb`) is measured for the indoor environment without eAmp for a UE – eNB/gNB distance of 12m, UL/DL frequency of 2400MHz/2490MHz and 5MHz bandwidth. The result of this measurement is shown in Fig. 4. Looking at the plots, the maximum RX power without eAmp is -70dBm. In order to compare this with the numerical analysis, we have recomputed the path loss and RX power updating the parameters based on the experimental settings. From the selected propagation models and experimental setup, this test case corresponds to femto cell propagation, and the new path loss is 71.97dB and RX power is indicated in Fig. 4, labeled as 'without eAmp-analytical', for different UHD gains. The plots in Fig. 4 indicate that the experimental RX power without eAmp is on average less than 15dB from the numerical result. This is mainly due to the difference in the theoretical and experimental output power from the iAmp of the SDR device used (see Table VI), and interference from other nearby LTE/WiFi transmissions at 2.4GHz band [6].

The experimental result without eAmp shows that we can achieve a coverage of 12m for UHD gains above 70dB, for QPSK and 16QAM modulation techniques. To extend the coverage and/or use higher modulation (such as 64QAM),

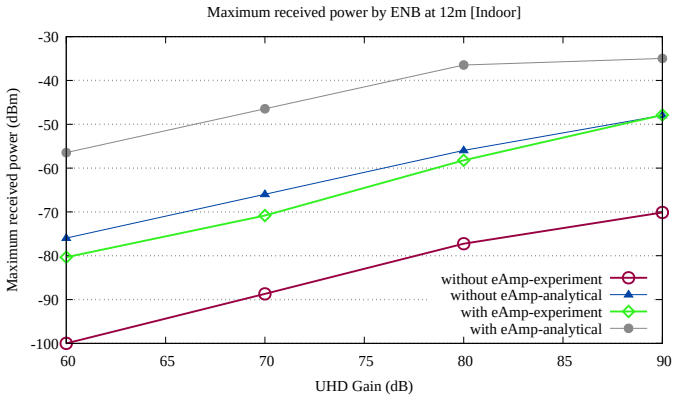

Fig. 4: Uplink received power at 12m [Indoor].

we add external component as discussed previously in section III-B. To specify the required external component, we update the numerical analysis based on our experimental parameter settings. As such, using the same antenna and SDR device gains, the final RX power is given by expressions in Table VII for path loss equal to 71.97dB. Consequently, considering the second testbed and receiver's sensitivity for the highest modulation (-86.3dB), we require an eAmp with minimum output power (Z) indicated in Table VII.

TABLE VII: Updated UL RX power and Z.

UHD gain (dB)	TX power (dBm)	RX power (dBm)	Z (dBm)
60	-43.91	$Z - 104.38$	18.08
70	-35.1	$Z - 95.57$	9.27
80	-18.9	$Z - 79.37$	–
90	-10.2	$Z - 70.67$	–

Following the above discussion, using eAmp described in section IV-A for the second testbed, we performed an experiment and illustrated the result in Fig. 4 with plots labeled 'with eAmp-experiment'. The result shows that, with eAmp, all the modulation techniques (discussed in this paper) can be performed with UHD gains as low as 60dB. In other words, it gives us a room to extend the S-RAN coverage into pico cell. This can be accomplished by increasing the UHD gains and/or performing lower modulation techniques as we extend the distance between UE and eNB/gNB.

2) Downlink TX and RX power: The TX power of eNB/gNB is measured without eAmp as a function of bandwidth (changing the number of physical resource blocks [PRBs]) as shown in Fig. 5. It depicts that eNB/gNB's maximum TX power is around -18dBm, much lower than UE. This is, on one hand, due to the same reasons stated for UE TX power, *i.e.,* hardware factors and full LTE protocol stack implementation. On the other hand, due to the larger PAPR at eNB/gNB than at UE. With eAmp, eNB/gNB's maximum TX power has increased from -20dBm to 3dBm.

The RX power at UE measured with respect to distance and bandwidth in both indoor and outdoor environments is illustrated in Fig. 6. For indoor experiment, the number of PRBs is set to 25 to measure the RX power against distance.

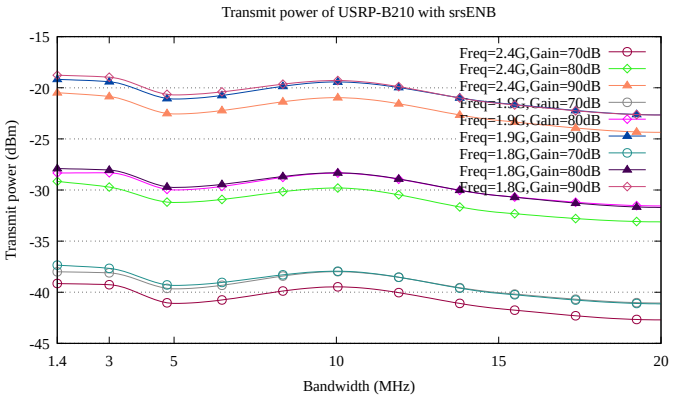

Fig. 5: TX power of USRP B210 with srsenb.

As shown in plot (1x1), the RX power decreases linearly with distance where we attain the lowest RX power when UE is placed 12m away from eNB/gNB. The maximum at 12m distance is -74.15dBm achieved with 90dB UHD gain for 1900MHz band. Comparing this with the numerical result, which is -33.45dBm using femto-cell model, there is a 40dB difference mainly due to the TX power of B210 contributing around 68% of RX power degradation. The measured RX power at 12m is sufficient to perform all the modulation techniques discussed above. The downlink coverage extension can be carried out in a similar fashion as the uplink as demonstrated previously. Moreover, as lower frequency bands indicate better received power than 2400MHz band, with lower frequency (1800MHz and 1900MHz bands), larger coverage can be obtained. Plot (1x2) shows the RX power against bandwidth, measured at 4m distance.

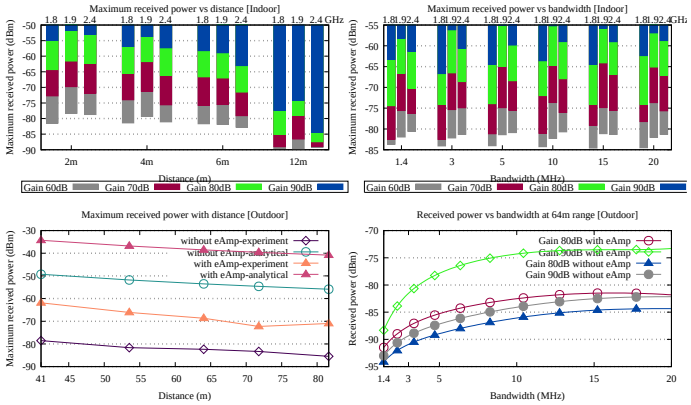

Fig. 6: Downlink received power.

Plot (2x1) in Fig. 6 shows RX power in outdoor environment as a function of distance. It's measured at 25 PRB and 90dB UHD gain. Without eAmp, the maximum RX power appears to be less than -80dBm for distances beyond 50m. In addition, there is a significant difference (more than 27dB) from the corresponding analytical result with micro-cell propagation model. More than 80% is contributed by the difference in the experimental and numerical TX power of B210. To enhance the received power and ultimately increase the coverage, we have to update the DL RX power using the experimental parameter settings and case 2 of the numerical analysis given in Table V. Since the distance measured in our experiment is 81m (which is less than $d_{\text{BP}} = 358.4m$), we use the path loss for case ($10m \leq d \leq d_{\text{BP}}$) of micro cell propagation model provided in Table II. The updated DL RX power and required Z is given in Table VIII. From the result, an eAmp with a minimum of 4 dBm output power is necessary to achieve the indicated distance and perform the three modulation techniques discussed above.

TABLE VIII: Updated DL RX power and Z.

UHD gain (dB)	TX power (dBm)	Path Loss	RX power (dBm)	Z (dBm)
90	-22.56	77.59	$Z - 90.15$	3.85

To support the above discussion, we conducted the experiment for the eAmp described in the second testbed. The obtained experimental result is shown in plot (2x1) of Fig. 6 labeled as 'with eAmp-experiment'. The maximum measured power is greater than -75dBm for distances beyond 80m. This result indicates that we can further increase the S-RAN coverage beyond 80m in outdoor. Similarly, the behaviour of RX power against bandwidth is shown in plot (2x2) measured at 64m, which shows a smooth variation of RX power with bandwidth in both with and without eAmp.

3) SNR: To study the performance of our model, we collected DL SNR at UE. Measurements were conducted while running `iperf3` network test tool to transmit random Transmission Control Protocol (TCP) traffics from `srsenb` (as a client) to `srsue` (as a server). Ten iperf3 trials were run, each for 10 seconds, and the average SNR were computed from recorded metrics file. The average SNR with respect to bandwidth, distance and MCS are plotted and shown in Fig. 7.

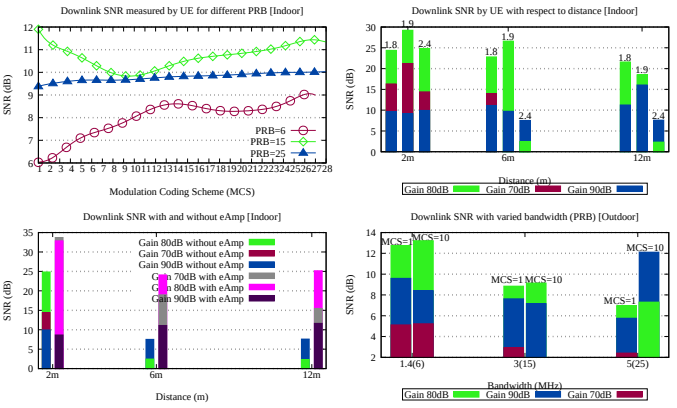

Fig. 7: Downlink SNR.

As Fig. 7 shows, there is clear difference in the SNR performance mainly due to distance and UHD gain. Although it's possible to attain the considered 12m indoor coverage without eAmp, the maximum SNR decreases from 24.8dB at [2m, 80dB, 2450MHz] to 2.3dB at [12m, 80dB, 2450MHz]. While this shows the performance degradation when the UE

moves further away from eNB/gNB, we can improve this result by changing UHD gain or employing eAmp. By increasing the UHD gain to 90dB, the SNR has increased to 7.6dB. This SNR result demonstrated comparable performance with the indoor SNR measurement reported by the work in [12]. Whereas, with eAmp, the corresponding performance has been enhanced to 25dB, which opens a door to increase the distance between UE and eNB/gNB. Extending the coverage can also be realized by setting other parameters. This can be seen from the behaviour of SNR performance as it varies with frequency, MCS, and PRB in addition to distance and UHD gain.

We also measured the SNR in outdoor environment within 64m range and 2450MHz frequency using the experiment setup shown in Fig. 2b. As shown in Plot (`2x2`) of Fig. 7, by changing the UHD gain setting, we observed upto 5dB SNR difference. Moreover, for higher MCSs such as 10, it's only possible to obtain good performance with UHD gains $\geq$80dB for PRBs 15 and 25. Even though this would result in a better throughput (since throughput is determined by the MCS and number of PRBs used), we require to lower the MCS and PRB to increase the coverage range. This can be observed from the higher SNR attained for MCS 1, where we have received a good signal for all PRB and UHD gain settings under test.

4) BLER: Since adding external components may lead to additional signal distortions, we measured signal performance in terms of BLER in addition to the SNR measurements presented previously. As discussed in the SNR measurement above, the eAmp has significantly improved the SNR at higher indoor (6m and 12m) and outdoor (64m) distances, hence, we opted to demonstrate the BLER performance at these distances. Other settings are set as: frequency at 2400MHz band, bandwidth of 5MHz (*i.e.,* PRB=25), and MCS = 1. The measured BLER for indoor and UHD gain at 80dB is shown in Fig. 8.

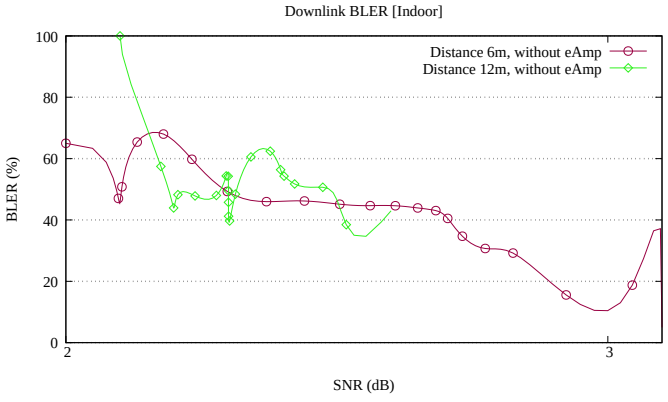

Fig. 8: Downlink BLER indoor.

As shown in Fig. 8, the BLER measurement shows only for the case without eAmp. This is because, the BLER measured with eAmp is zero (0%) for all UHD gains and all indoor distances considered. This is true as the SNR measured with eAmp is above 10dB even for lower UHD gains (see discussion in section IV-B3). However, without eAmp, the BLER lowers as the SNR increases.

The BLER is also measured in outdoor environment and is plotted as shown in Fig. 9. The measurement is conducted for UHD gains 70dB, 80dB and 90dB. The result shows, for lower UHD gains, the obtained SNR is very low and gives very high BLER. For higher UHD gains, the BLER gets very close to zero with some fluctuations for 80dB UHD gain.

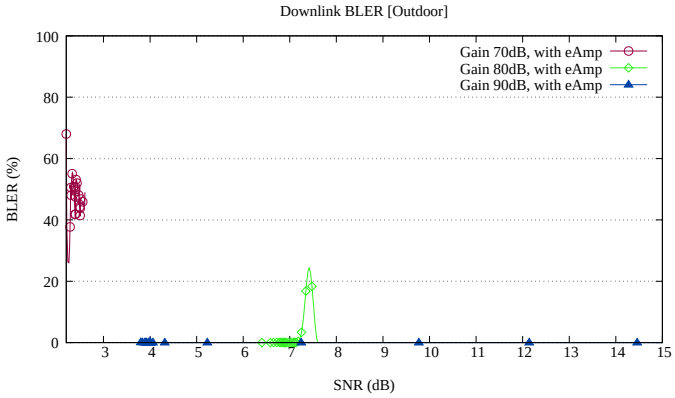

Fig. 9: Downlink BLER outdoor with eAmp.

As the plots in Fig. 8 and 9 illustrates and the discussion thereof, the BLER, like the SNR, depends mainly with distance and UHD gain. No significant signal distortion has been observed with the added eAmp. Rather the eAmp improved the SNR with constant gain (20dB at 2400MHz band) and hence provided lower BLER. This is true based on the fact that, as shown in plot (`2x1`) of Fig. 6, the used eAmp (EVAL-CN0417-EBZ) provided nearly linear output gain. In addition, the extra internal amplifier (PGA-102+) used inside USRP-B210 is also a constant gain power amplifier with low noise figure and better linearity [27]. Consequently, the observed signal performance variations due to UHD gains raises from the gains added by the internal components of the USRP-B210 SDR including mixers and amplifiers of AD9361/AD9364 RFIC. Thus, gain of these components could be configured to avoid any signal distortion and non-linearities [25].

V. Conclusions

This paper presented numerical and experimental analysis of extending 3GPP 4G/5G S-RAN cell coverage. Communication between UE and eNB/gNB has been modeled using SDR platform as radio transceiver in UL and DL directions. This model is used to numerically analyze the final RX power using different propagation models standardized for 4G/5G networks. A testbed was prepared using srsLTE software and USRP B210 SDR device to validate the numerical analysis. Then, experiments were conducted to evaluate the performance of S-RAN model in terms of TX power, RX power, SNR and BLER in both indoor and outdoor environments. The numerical analysis has suggested that with proper design of SDR transceiver (antenna selection, eAmp and/or eLNA+eFil), macro-cell propagation could be achieved. This has been

experimentally demonstrated using eAmp where cell coverage has been improved from indoor femto-cell to small micro-cell in outdoor. Thus, the obtained numerical and experimental results proved that 4G/5G S-RAN cell coverage can be extended to a large micro-cell and macro-cell by designing and adding external equipment on SDR platforms.

The UE and eNB/gNB in our testbed were placed in LOS and are stationary. For future work, we plan to experiment our model for mobile UE and eNB/gNB and in non-LOS conditions. In addition, the S-RAN model presented in this paper can also be tested using other 4G/5G implementations such as OAI and other SDR devices.

REFERENCES

[1] 3GPP, "3rd Generation Partnership Project (3GPP)," [Accessed: March 2021]. [Online]. Available: https://www.3gpp.org/

[2] LTE, "LTE," [Accessed: March 2021]. [Online]. Available: https://www.3gpp.org/technologies/keywords-acronyms/98-lte

[3] LTE-A, "LTE-Advanced," [Accessed: March 2021]. [Online]. Available: https://www.3gpp.org/technologies/keywords-acronyms/97-lte-advanced

[4] LTE-A Pro, "LTE-Advanced Pro," [Accessed: March 2021]. [Online]. Available: https://www.3gpp.org/news-events/1745-lte-advanced_pro

[5] 5G, "5G NR," [Accessed: March 2021]. [Online]. Available: https://www.3gpp.org/lte-2

[6] I. Gomez-Miguelez, A. Garcia-Saavedra, P. D. Sutton, P. Serrano, C. Cano, and D. J. Leith, "srsLTE: An open-source platform for LTE evolution and experimentation," *Proceedings of the Annual International Conference on Mobile Computing and Networking, MOBICOM*, vol. 03-07-Octo, pp. 25–32, 2016.

[7] F. Kaltenberger, A. P. Silva, A. Gosain, L. Wang, and T.-T. Nguyen, "Openairinterface: Democratizing innovation in the 5g era," *Computer Networks*, vol. 176, p. 107284, 2020.

[8] "Openlte: an open source implementation of the 3gpp lte specifications." [Accessed: December 2020]. [Online]. Available: http://openlte.sourceforge.net/

[9] Amarisoft, "Software company dedicated to 4G and 5G," [Accessed: February 2021]. [Online]. Available: https://www.amarisoft.com/

[10] USRP-B210, "Universal Software Radio Peripheral (USRP)," [Accessed: October 2020]. [Online]. Available: https://kb.ettus.com/B200/B210/B200mini/B205mini

[11] EURECOM, "EXPRESSMIMO2," [Accessed: March 2020]. [Online]. Available: http://openairinterface.eurecom.fr/expressmimo2

[12] A. Issa, N. Hakem, N. Kandil, and A. Chehri, "Performance analysis of mobile network software testbed," in *Human Centred Intelligent Systems*. Springer, 2021, pp. 305–319.

[13] F. Gringoli, P. Patras, C. Donato, P. Serrano, and Y. Grunenberger, "Performance assessment of open software platforms for 5g prototyping," *IEEE Wireless Communications*, vol. 25, no. 5, pp. 10–15, 2018.

[14] A. Hematian, J. Nguyen, C. Lu, W. Yu, and D. Ku, "Software defined radio testbed setup and experimentation," in *Proceedings of the International Conference on Research in Adaptive and Convergent Systems*, 2017, pp. 172–177.

[15] B. Home eNode, "3rd generation partnership project; technical specification group radio access network; evolved universal terrestrial radio access (e-utra); fdd home enode b (henb) radio frequency (rf) requirements analysis," 2012.

[16] 3GPP TR36.931, "3rd Generation Partnership Project;Technical Specification Group Radio Access Network; Evolved Universal Terrestrial Radio Access (E-UTRA); Radio Frequency (RF) requirements for LTE Pico NodeB (Release13)," vol. V13.0.0, Jan. 2016.

[17] Report ITU-R M.2292-0, "Characteristics of terrestrial IMT-Advanced systems for frequency sharing/interference analyses." vol. M Series, Dec. 2013. [Online]. Available: https://www.itu.int/dms_pub/itu-r/opb/rep/R-REP-M.2292-2014-PDF-E.pdf

[18] ITU-R P.1238-10, "Propagation data and prediction methods for the planning of indoor radiocommunication systems and radio local area networks in the frequency range 300 MHz to 450 GHz P Series Radiowave propagation," vol. P Series R, 2012.

[19] 3GPP TR 36.873, "Study on 3D channel model for LTE," vol. v. 12.0.0, Jul. 2015.

[20] 3GPP TR 38.901, "Study on channel model for frequencies from 0.5 to 100 GHz," vol. v. 14.3.1, May 2017.

[21] D. Martin-Sacristan, J. F. Monserrat, J. Cabrejas-Penuelas, D. Calabuig, S. Garrigas, and N. Cardona, "On the way towards fourth-generation mobile: 3gpp lte and lte-advanced," *EURASIP journal on wireless communications and networking*, vol. 2009, pp. 1–10, 2009.

[22] 3GPP, "LTE; Evolved Universal Terrestrial Radio Access (E-UTRA); Base Station (BS) radio transmission and reception (3GPP TS 36.104 version 14.3.0 Release 14)," vol. 0, 2017.

[23] Analog Devices, "USB Powered 2.4 GHz RF Power Amplifier," *Circuit Note*, 2020. [Online]. Available: https://www.analog.com/media/en/reference-design-documentation/reference-designs/CN0417.pdf

[24] USRP B210, "RF performance data." [Accessed: November 2020]. [Online]. Available: https://kb.ettus.com/images/c/cb/B200_RF_Performance.pdf

[25] M. W. O'Brien, J. S. Harris, O. Popescu, and D. C. Popescu, "An experimental study of the transmit power for a usrp software-defined radio," in *2018 International Conference on Communications (COMM)*, 2018, pp. 377–380.

[26] R. Zitouni and L. George, "Output power analysis of a software defined radio device," in *2016 IEEE Radio and Antenna Days of the Indian Ocean (RADIO)*, 2016, pp. 1–2.

[27] PGA102, "Ultra High Dynamic Range Monolithic Amplifier PGA-102+," [Accessed: October 2020]. [Online]. Available: hhttps://www.minicircuits.com/pdfs/PGA-102+.pdf